DIFFUSIVE LANGEVIN DYNAMICS OF MODEL ALKANES *

Ronald M. LEVY, Martin KARPLUS
Department of Chemistry, Harvard University, Cambridge, Massachusetts 02138, USA

and

J. Andrew McCAMMON
Department of Chemistry, University of Houston, Houston, Texas 77004, USA

Received 15 May 1979; in final form 25 June 1979

The diffusive Langevin equation of motion is used to simulate the equilibrium and dynamic properties of model alkanes for times up to 100 ns. Comparisons are made between the results obtained with an isolated molecule potential surface and with one modified to incorporate solvent effects.

1. Introduction

Molecular dynamics simulations have become a popular and powerful tool for the study of problems involving the interactions of many particles. Most of the applications have been to equilibrium and dynamic properties of condensed phases [1] although recently the technique has been employed to simulate the motions of the 458 heavy atoms of a single protein molecule in the neighborhood of its native structure [2]. For many processes of interest in liquids and in proteins the relaxation times are too long for a full molecular dynamics approach. It is often possible to simplify such problems by separating a large system into two parts, only one of which is studied in detail. The most obvious case is a solute at infinite dilution; only the solute atoms are explicitly retained in the hamiltonian, and the effect of the solvent atoms is incorporated into the dynamics by the use of an effective solute potential, by the presence of a random force term and by frictional damping. Such a "subsystem plus heat bath" separation of the many-particle problem is termed brownian or stochastic dynamics [3–8].

In this report, we present the results of stochastic dynamic calculations in the diffusive limit [4] for butane and heptane in aqueous solution. Processes with relaxation times ranging from 0.1 to 100 ps are evaluated by simulations extending over 100 ns. Particular attention is focused on the molecular potential energy function, which includes effects of the solvent and external constraints on the equilibrium and dynamic properties of the hydrocarbon chains. The behavior of these chains, which is of intrinsic interest, can serve as a model for relaxation in lipid membranes and in aliphatic amino acid side chains.

* Supported in part by grants from the National Institutes of Health and the National Science Foundation.

2. Method

The equation of motion descriptive of brownian particles is the Langevin equation [9]

$$m_i \, \mathrm{d}\mathbf{v}_i/\mathrm{d}t = -\beta_i \mathbf{v}_i + F_i + A_i(t) , \qquad (1)$$

where m_i, $\mathbf{v}_i$ and β_i are the mass, velocity and friction constant of the ith particle and F_i is the systematic force acting on the ith particle due to the potential of mean force; F_i in general depends on the coordinates of all of the particles. The stochastic term, $A_i(t)$ represents the randomly fluctuating force on the particle due to the solvent; it is assumed to have a gaussian distribution with first and second moments

$$\langle A_i(t)\rangle = 0\,,$$

$$\langle A_i(t)\cdot A_j(t')\rangle = 6\beta_i kT\delta(t-t')\,\delta_{ij}\,. \qquad (2)$$

In the diffusive regime, the particle momenta relax to equilibrium much more rapidly than the displacements. With the assumption that the forces are slowly varying (i.e., that it is possible to take time steps large compared to the momentum relaxation time ($\Delta t \gg m_i/\beta_i$)), eq. (1) can be integrated twice to obtain the equation [4,5,9] for the displacement vector, r_i,

$$r_i(t+\Delta t) = r_i(t) + [F_i(t)/\beta_i]\,\Delta t + \Delta r_i(t)\,. \qquad (3)$$

The term $\Delta r_i(t)$ is the random displacement due to the stochastic force; from eq. (2) it is chosen from a gaussian distribution with zero mean and second moment $6D_i\,\Delta t$, where D_i, the diffusion coefficient, is kT/β_i.

Eq. (3) is the equation that was used to calculate the trajectories of the hydrocarbon chains. An extended-atom model was introduced, in which the CH_3 and CH_2 units are represented as spheres of van der Waals radius 1.85 Å; the bond lengths and angles of the alkane chains were set equal to 1.523 Å and 111.3°, respectively. Each extended atom group along the chain acted as a point center of frictional resistance with a Stokes law friction constant ($\beta = 6\pi a\eta$). To determine β, the viscosity of water at 25°C ($\eta = 0.01$ poise) was used and a was set equal to the extended atom van der Waals radius; with these parameters, $\beta = 3.45 \times 10^{-9}$ g/s. This is to be compared with the value $\beta = 2.2 \times 10^{-9}$ g/s obtained from the experimental diffusion coefficient of methane in water at 25°C.

3. Potential function

The negative gradient of the potential of mean force is used for F_1 in eqs. (1) and (3). This is a combination of the potential energy arising from the interaction among the particles composing the solute molecule and the effective potential due to the solvent molecules. The molecular potential was expressed as a sum of two types of terms; the first is a torsional potential energy for each of the dihedral angles, and the second consists of pair-wise Lennard-Jones interactions, between extended atoms separated by four or more bonds [4,10–12]. For butane there is one angular degree of freedom and only the associated torsional potential was used, but for heptane both torsional and nonbonded terms are required.

The solvent contribution to the torsional nonbonded potential was obtained from the work of Pratt and Chandler [12], which expresses the potential due to the solvent as $-kT\ln y$, where y is the cavity distribution function. For the torsional potential $\ln y(\phi)$ was estimated from a pseudo-diatomic cavity model for butane with each ethyl group replaced by a sphere at the midpoint of the ethyl C–C bond [12]. The isolated molecule [$V_{\mathrm{mol}}(\phi)$], and solvent modified potential [$V_{\mathrm{mol}}(\phi) + V_{\mathrm{sol}}(\phi)$] are compared in fig. 1a. It is clear that the main difference between the two potentials is a stabilization of the gauche configuration by the solvent. The differences in energy at 25°C between the trans and gauche geometry in the vacuum and in the solvent are 0.70 kcal/mole and 0.16 kcal/mole, respectively. For the solvent effect on the nonbonded interaction, the cavity distribution function for two methane molecules dissolved in water was used

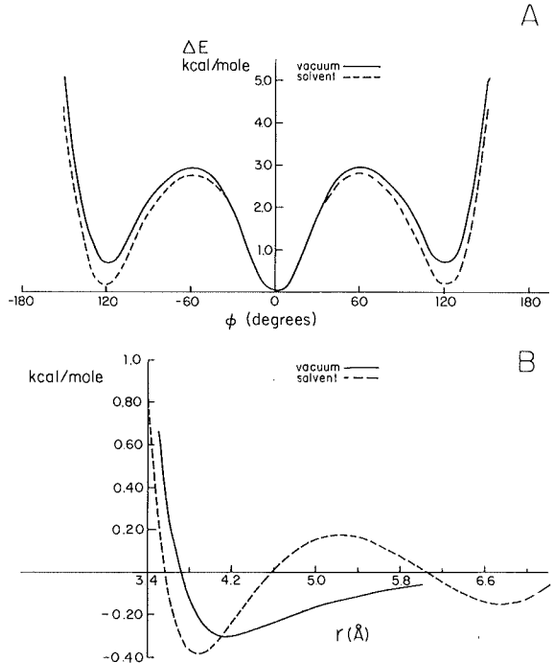

Fig. 1. (A) Alkane, intramolecular torsional potential in vacuum and in water at 25°C. (B) Lennard-Jones potential between heptane atoms separated by four or more bonds in vacuum, and in water at 25°C.

[12]; the isolated system and solvent modified potentials are shown in fig. 1b. The latter has a slightly deeper energy minimum (–0.38 versus 0.30 kcal/mole), which occurs at a smaller interparticle separation (3.9 versus 4.15 Å); at larger separations the attraction is more quickly screened in the solvent.

To model hindered dihedral angle motion, expected in amino acids that are part of a protein or hydrocarbons that are part of a membrane, a heptane trajectory was calculated with the three atoms at one end of the chain held stationary. There are four dihedral angles in heptane, all of which can vary if three end atoms are fixed. However, motion of four atoms contributes to a change in the dihedral angle (ϕ_4) at the unrestricted end of the molecule, while the dihedral angle (ϕ_1) closest to the restricted end changes only as a result of the motion of a single atom.

4. Calculations

For all of the systems considered, eq. (3) was integrated in cartesian coordinates with the bond lengths and angles of the molecule constrained to the initial value by use of the SHAKE algorithm [10]. In general, a correction term should be introduced when the Langevin equation is solved with constraints [7,13]. This term was omitted from the present simulation in which the effect is expected to be small. Analytic evaluation of the metric tensor correction for butane indicates that the relative populations in the significant trans, gauche, and transition state configurations would be changed by 10% or less; only in the energetically forbidden cis region would the effect be important. Further a simulation of butane in the absence of the torsional potential demonstrated that the actual correction for the SHAKE algorithm is even smaller than that calculated from the metric tensor.

For the butane simulation, time steps of 0.005 ps and 0.05 ps were compared; for the other molecules, time steps between 0.025 and 0.05 ps were used. Butane trajectories were run for 90 ns (25°C) and 20 ns (50°C) on the solvent modified potential surface and 20 ns (25°C) on the vacuum molecular potential surface. Heptane trajectories on the solvent modified surface (25°C) were recorded for 20 ns without constraints and 10 ns with three atoms held fixed. 10 ns of the butane trajectory required 15 min CPU time on an IBM 370/168 computer.

5. Results

To test the method, the stochastic trajectories for butane were used to evaluate the equilibrium distribution, which can be compared with that obtained directly from the configurational partition function. The equilibrium fractions of trans and gauche states predicted by the latter are listed in table 1; the vacuum result at 25°C and the results in water at 25°C and 50°C are given. For comparison the values obtained with a three-state rotational isomeric model of butane are included; the two sets of values differ by about 10%. At 25°C in vacuum, butane is 65% trans and 35% gauche (K_{eq} = 0.54), whereas in water at the same temperature butane is predicted to be 44% trans and 56% gauche (K_{eq} = 1.27). The predicted fractions of trans and gauche states of butane in water are nearly the same at 25°C and 50°C because, the temperature effect on the vacuum distribution is approximately cancelled by the solvent contribution.

The equilibrium results obtained from the butane trajectories by determining the fraction of the time spent in each of the regions (T, G+, G–) are also given in table 1. It can be seen that there is good agreement with the values calculated directly. Figs. 2a and 2b show the angular distributions obtained from trajectories on the vacuum surface and on the solvent-modified surface. There is good agreement with the configurational partition function results, not only for the peak heights but also for the angular distributions within each well; the distribution is slightly less smooth in the 20 ns run due to greater statistical fluctuations. The comparison indicates that a time step of 0.05 ps provides an accurate sample of the rotational potential. This is in accord with the small difference between the results obtained with 0.005 ps and 0.05 ps time steps.

The distributions of heptane rotational isomers obtained from the 20 ns trajectory and the rotational isomeric model are also listed in table 1. It can be seen that due to the presence of nonbonded interactions there is an increase in trans isomers, relative to butane. The disagreement between the trajectory and rotational isomeric model calculations as to whether ϕ_1, ϕ_4 or ϕ_2, ϕ_3 is more trans may arise because the trajectory values are not completely converged.

Table 1
Equilibrium distribution of butane and heptane

	Vacuum potential, 25°C			Solvent potential					
				25°C			50°C		
	T	G+	G–	T	G+	G–	T	G+	G–
Butane									
configurational partition function	65	17.5	17.5	44	28	28	43	27.5	27.5
rotational isomeric model	62	19	19	40	30	30	38	31	31
trajectories									
stepsize 0.005 ps duration 7 ns				45	27	28			
stepsize 0.05 ps duration 90 ns				43	30	27			
stepsize 0.05 ps duration 20 ns	65	21	14				40	38	22
Heptane									
rotational isomeric model									
ϕ_1, ϕ_4				47	26.5	26.5			
ϕ_2, ϕ_3				50	25	25			
trajectory									
stepsize 0.05 ps duration 21 ns									
ϕ_1, ϕ_4				50	27	23			
ϕ_2, ϕ_3				47	28	25			

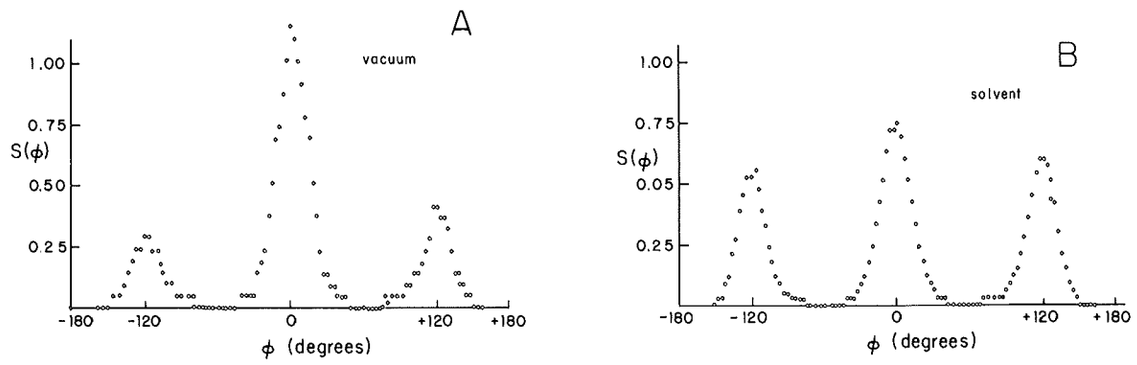

Fig. 2. Butane rotational distributions obtained from trajectories: (A) 20 ns simulation on the vacuum surface, and (B) 90 ns simulation on the solvent modified surface.

6. Dynamics

The internal dynamics of interest for these hydrocarbon chains separate into two very different time scales. The shorter, on the order of tenths of picoseconds, corresponds to the torsional oscillations within a potential well (gauche or trans) and the longer, on the order of a hundred picoseconds, is associated with the transitions from one potential well to another. To probe both of these it is helpful to introduce the appropriate time correlation functions [14,15].

We consider butane in detail because the equilibrium results are close to the predicted values and the dynamics can be compared directly with standard models for reaction rates. To illustrate the dynamic behavior, part of a trajectory that includes oscillations within a well (T) and one transition over a barrier (G− → T) is shown in fig. 3. It is clear that the molecule spends most of the time oscillating in a well and makes a rather rapid transition over the barrier, although diffusional behavior at the top of the barrier is evident.

For motion within a given well, the relaxation time can be calculated within the harmonic approximation [9]; the local oscillatory motion is predicted to be overdamped with a relaxation time of 0.15 ps. For the trajectory results, the corresponding relaxation time can be obtained from the correlation function, $C_\phi(\tau) = \langle \Delta\phi(t)\, \Delta\phi(t+\tau)\rangle_t$ shown in fig. 4, where $\Delta\phi(t)$ is the value of the butane dihedral angle relative to the average, $\phi = 0$. With an exponential fit to $C_\phi(\tau)$, the relaxation time is 0.17 ps from the trajectory with 0.05 ps stepsize and 0.21 ps from the trajectory with a 0.005 ps stepsize.

To analyse the butane isomerization kinetics, we make use of the phenomenological rate equations for the decay in the fluctuations of the numbers of trans and gauche isomers from the equilibrium values. The relaxation time for the fluctuation in the number of trans particles is $\tau = (2K_{T\to G} + K_{G\pm\to T})^{-1}$, where the

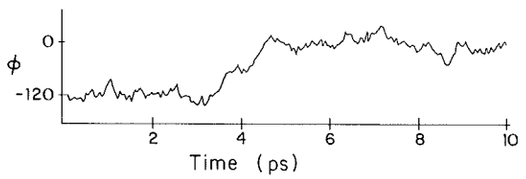

Fig. 3. 10 ps segment of a butane trajectory showing one transition over the barrier (G− → T) at about 4 ps.

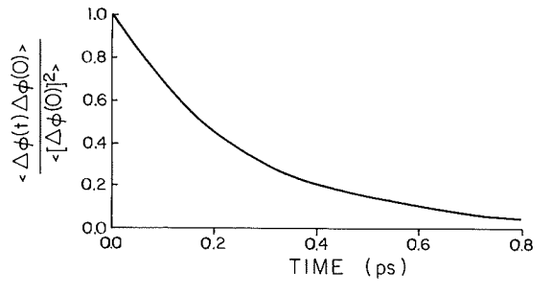

Fig. 4. Butane rotational autocorrelation function of torsional oscillations within the trans well; $\Delta\phi(t)$ is the value of the butane dihedral angle relative to the average, $\phi = 0$.

K are isomerization rate constants and τ can be evaluated from the correlation function, $C_N(\tau) = \langle \delta N(t) \times \delta N(t+\tau)\rangle_t$ [14,15]; an alternative method of analysis uses first-passage time statistics [6]. The butane rate constants $2K_{T\to G\pm}$ and $K_{G\pm\to T}$ obtained from the calculated values of τ and the equilibrium constant (K_{eq}) are listed in table 2. The T → G± isomerization rate is faster with the solvent-modified potential than in vacuum and the back reaction is slower.

The most straightforward procedure to obtain isomerization rates might seem to be to count the number of barrier crossings and divide by the total duration of the simulation. However, this method is difficult to use for diffusive trajectories because a molecule frequently recrosses the barrier several times before falling into one or another well (see fig. 3). Such behavior corresponds to the transmission coefficient being less than unity in transition state theory [16]. In practical terms, the rate becomes strongly dependent on the time elapsed between conformations included in the sample; estimates of τ varied between 19 and 132 ps as the elapsed time increased from 0.1 ps to 100 ps.

To compare the trajectory results with simple models for reaction rates, the butane isomerization is idealized to the motion over a barrier of a single particle in a one-dimensional potential coupled to heat bath. For this case, Kramers' classical diffusion treatment [17] yields

$$K_{T\to G\pm}\,(\text{Kramers}) = (\omega_T \omega_{TS}/2\pi)(I_{TS}/\beta_{rot}^{TS}) \exp(-\Delta E^*/kT)\,, \qquad (4)$$

where ΔE^* is the barrier height, ω_T and ω_{TS} are the vibrational frequencies at the bottom of the trans well

Table 2
Butane isomerization rate constants (s^{-1})

Model	Vacuum potential (25°C)		Solvent potential (25°C)	
	$2K_{T\to G\pm}$	$K_{G\pm\to T}$	$2K_{T\to G\pm}$	$K_{G\pm\to T}$
trajectory results	7.6×10^9	1.4×10^{10}	9.3×10^9 (1.0×10^{10}) a)	6.4×10^9 (8.3×10^9) a)
classical transition state theory [eq. (5), $\kappa=1$]	4.6×10^{10}	8.3×10^{10}	5.9×10^{10}	4.5×10^{10}
Kramers transition state theory [eq. (4)]	9.6×10^9	1.8×10^{10}	1.0×10^{10}	8.1×10^9

a) Obtained from trajectory with 0.005 ps stepsize; all other trajectory results use a stepsize of 0.05 ps.

and at the top of the inverted barrier and β_{rot}^{TS} and I_{TS} are the torsional friction constant and moment of inertia of butane in the transition configuration; the value of $\beta_{rot} = 9.1\times10^{-2}$ g cm^2 s^{-1} mole^{-1}. The classical transition state theory formula [16] for the reaction rate is

$$K_{T\to G\pm}(\mathrm{TST}) = \kappa(\omega_T/2\pi)\exp(-\Delta E^*/kT), \qquad (5)$$

where κ is the transmission coefficient; comparing eqs. (4) and (5) we see that $\kappa = \omega_{TS} I_{TS}/\beta_{rot}^{TS}$ in the Kramers model. Table 2 lists the rate constants for the butane isomerization obtained from eqs. (4) and (5); if the frequency factor kT/h is used, the rates are increased two-fold over the classical values. The rate constants from the Kramers model, which are about five times smaller than the transition state values, are in good agreement with the trajectory results. Since diffusive dynamics [eq. (3)] was assumed in the trajectory calculations, the differences between the Kramers and trajectory results must be due to approximations [18] in applying the former or to lack of convergence in the latter. As to the validity of the diffusive limit for butane isomerization in water, it depends on the collisional damping of the torsional motion. The effective collision frequency [19,20] is $\beta_{rot}/I_{rot} = 7.4\times10^{13}$ s^{-1}, about half that corresponding to the monomer (CH_4) friction coefficient. The critical quantity determining the validity of the diffusion limit is the number of collisions that occur during the barrier crossing. For the present case, this quantity is $2\pi\beta_{rot}^{TS}/I_{TS}\omega_{TS} \approx 35$, a value in the range for which recent analyses [20,21] have shown that the diffusion limit is appropriate. However, further work is necessary to determine the validity of the present model that uses the friction coefficient obtained from the translational diffusion coefficient of a monomer unit in the Langevin equation for the polymer dynamics.

With the Kramers model, we can analyse the effect

Table 3
Heptane dynamics, unconstrained

ϕ	Number of transitions in 21 ns a)			Isomerization rate constant b)		Relaxation time of angular correlation function c)
	total	T→G+	T→G−	$2K_{T\to G\pm}$	$K_{G\pm\to T}$	
1	166	44	40	6.1×10^9	7.4×10^9	94
2	119	28	33	5.2×10^9	4.8×10^9	134
3	121	31	28	4.1×10^9	4.1×10^9	148
4	141	35	40	6.7×10^9	6.5×10^9	108
1, 4 average	154	40	40	6.4×10^9	7.0×10^9	101
2, 3 average	120	30	31	4.7×10^9	4.5×10^9	141

a) 5.0 ps intervals between sampling the trajectory.
b) Obtained from evaluation of $\langle\delta N_T(\tau)\,\delta N(0)\rangle$; rate s^{-1}.
c) Obtained from evaluation of $\langle\cos[\phi(\tau)-\phi(0)]\rangle$, time in ps.

Table 4
Heptane dynamics, constrained

ϕ	Number of transitions in 10 ns [a]			Isomerization rate constant [b]		Relaxation time of angular correlation function [c]
	total	T → G+	T → G−	$2K_{T\to G\pm}$	$K_{G\pm\to T}$	
1	6	2	1			
2	16	5	4			
3	15	5	3	(6.5×10^8)	(1.8×10^9)	700
4	71	18	18	(1.0×10^{10})	(5.7×10^9)	101

a) 5.0 ps intervals between sampling the trajectory.
b) Obtained from evaluation of $\langle \delta N_T(\tau)\, \delta N(0)\rangle$; rate s^{-1}; the values in parentheses are estimates.
c) Obtained from evaluation of $\langle \cos[\phi(\tau) - \phi(0)]\rangle$, time in ps.

of the differences in the shape of the vacuum and solvent-modified potentials on the rate constant. The 0.15 kcal/mole lower T → G± barrier in water increases the rate constant by a factor of 1.29, while the smaller curvature of the rotational barrier in water decreases the rate constant by a factor of 1.17. The overall result is a small increase (by a factor of 1.09) of $K_{T\to G\pm}$ in water. There is a larger effect on the rate constant $K_{G\pm\to T}$, where both factors are in the same direction.

For heptane, free and with three atoms constrained, the dynamic results are given in tables 3 and 4, respectively. We list the number of isomerization transitions for each of the angles and, where sufficient trajectory simulation data were obtained, the isomerization rate constants calculated from $C_N(\tau)$ and the relaxation time for the angular correlation function, $\langle \cos[\phi(t+\tau) - \phi(t)]\rangle_t$. For unconstrained heptane the isomerization rates are between 1.5 and 2 times slower than in butane. Further, the rates for the outer dihedral angles are significantly greater than those for the inner angles, though still less than for butane. The number of transitions and the angular correlation function show a corresponding difference in mobility between the outer and inner dihedral angles. That the angular correlation function relaxation times are shorter than the reciprocal of the rate constants is due to the fact that motion within a given well contributes to its decay as well as the transition between wells. In the constrained heptane chain, there is a large difference in mobility among the torsional angles; e.g., there were ten times as many transitions for ϕ_4 as compared with ϕ_1. Plots of the angular correlation function for each of the dihedral angles given in fig. 5 show this striking difference in behavior. While the motion of ϕ_4, is comparable to the free heptane chain, ϕ_3 relaxes about five-fold slower than in the unconstrained simulation.

This preliminary study of the dynamics of butane and heptane has demonstrated that diffusive Langevin dynamics simulations are an important tool for the study of intramolecular motions occurring on widely separated time scales. In future work the method will be used to calculate specific motional parameters for comparison with experiment (e.g., NMR relaxation

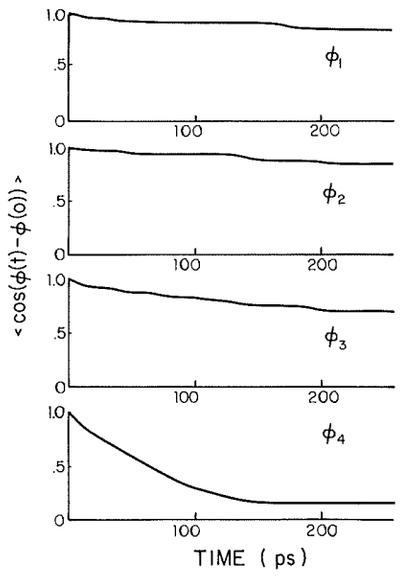

Fig. 5. Angular correlation functions for each of the dihedral angles from the constrained heptane trajectory. First three atoms are stationary.

times [22,23]). Of particular interest are the constrained chain dynamics, which have important implications for the motional behavior expected for amino acid side chains of proteins and hydrocarbon chains in lipid membranes.

Acknowledgement

We thank Lawrence Pratt, James Skinner and Peter Wolynes for helpful discussions. We are grateful to Carl Moser and the Centre Européen de Calcul Atomique et Moléculaire (Orsay, France), where most of the computations were done, for hospitality and support at the 1978 summer workshop.

References

[1] B.J. Alder and W.G. Hoover, in: Physics of simple liquids, eds. H.N.V. Temperley, J.S. Rowlinson and G.S. Rushbrooke (Elsevier, Amsterdam, 1968) ch. 4.
[2] J.A. McCammon, B.R. Gelin and M. Karplus, Nature 267 (1977) 585.
[3] P. Turq, F. Lantelme and H.L. Friedman, J. Chem. Phys. 66 (1977) 3039.
[4] D.L. Ermak and J.A. McCammon, J. Chem. Phys. 69 (1978) 1352.
[5] D.L. Ermak, J. Chem. Phys. 62 (1975) 4189.
[6] E. Helfand, J. Chem. Phys. 69 (1978) 1010.
[7] M. Fixman, J. Chem. Phys. 69 (1978) 1527.
[8] M. Fixman, J. Chem. Phys. 69 (1978) 1538.
[9] S. Chandrasekhar, Rev. Mod. Phys. 15 (1943) 1.
[10] J.P. Ryckaert, G. Cicotti and H.J.C. Berendsen, J. Comp. Phys. 23 (1977) 327.
[11] J.P. Ryckaert and A. Bellemans, Chem. Phys. Letters 30 (1975) 123.
[12] L.R. Pratt and D. Chandler, J. Chem. Phys. 67 (1977) 3683.
[13] M.R. Pear and J.H. Weiner, Brownian Dynamics Study of a Polymer Chain of Linked Rigid Bodies, J. Chem. Phys., submitted for publication.
[14] R. Zwanzig, Ann. Rev. Phys. Chem. 16 (1965) 67.
[15] D. Chandler, J. Chem. Phys. 68 (1978) 2959.
[16] S. Gladstone, K. Laidler and H. Eyring, The theory of rate processes (McGraw-Hill, New York, 1941).
[17] H.A. Kramers, Physica 7 (1940) 284.
[18] S.H. Northrup and J.T. Hynes, J. Chem. Phys. 69 (1978) 5246.
[19] D. Chandler, J. Chem. Phys. 62 (1975) 1358.
[20] J.A. Montgomery, D. Chandler and B.J. Berne, J. Chem. Phys. 70 (1979) 4056.
[21] J. Skinner and P. Wolynes, J. Chem. Phys. 69 (1978) 2143.
[22] R.J. Wittebort and A. Szabo, J. Chem. Phys. 69 (1978) 1722.
[23] R.E. London and J. Avitable, J. Am. Chem. Soc. 99 (1977) 7765.